Original Article

Intravoxel incoherent motion diffusion-weighted imaging for early assessment of combined anti-angiogenic/chemotherapy for colorectal cancer liver metastases

Huita Wu[1,2,3#], Bangkai Li[4#], Zike Yang[1#], Haonan Ji[1], Yifang Guo[5], Jianzhong Lin[6], Xin Wang[1]

[1]Department of Oncology, Zhongshan Hospital of Xiamen University, School of Medicine, Xiamen University, Xiamen, China; [2]Fujian Provincial Key Laboratory of Chronic Liver Disease and Hepatocellular Carcinoma, Zhongshan Hospital of Xiamen University, School of Medicine, Xiamen University, Xiamen, China; [3]The Third Clinical Medical College, Fujian Medical University, Fuzhou, China; [4]Emergency Department (Outpatient Chemotherapy Center), The Third Affiliated Hospital of Kunming Medical University/Yunnan Cancer Hospital, Kunming, China; [5]Department of Oncology and Hematology, Xiamen Haicang Hospital, Xiamen, China; [6]Department of Magnetic Resonance Imaging, Zhongshan Hospital of Xiamen University, School of Medicine, Xiamen University, Xiamen, China

Contributions: (I) Conception and design: X Wang, J Lin; (II) Administrative support: X Wang, H Wu, J Lin; (III) Provision of study materials or patients: H Wu, B Li, Z Yang, H Ji, Y Guo; (IV) Collection and assembly of data: H Wu, B Li, Z Yang, H Ji, Y Guo; (V) Data analysis and interpretation: H Wu, B Li, Z Yang; (VI) Manuscript writing: All authors; (VII) Final approval of manuscript: All authors.

[#]These authors contributed equally to this work.

Correspondence to: Xin Wang, MD. Department of Oncology, Zhongshan Hospital of Xiamen University, School of Medicine, Xiamen University, 201 Hubin South Road, Siming District, Xiamen 361004, China. Email: szzj1997@163.com; Jianzhong Lin, BMed. Department of Magnetic Resonance Imaging, Zhongshan Hospital of Xiamen University, School of Medicine, Xiamen University, 201 Hubin South Road, Siming District, Xiamen 361004, China. Email: xmzshljz123@163.com.

Background: To explore the value of intravoxel incoherent motion diffusion-weighted imaging (IVIM-DWI) in the early assessment of colorectal cancer liver metastases (CRLM).

Methods: A total of 34 patients with pathologically confirmed unresectable CRLM were enrolled. All participants uniformly received capecitabine and oxaliplatin (CAPOX) plus bevacizumab chemotherapy as standard first-line treatment for advanced colorectal cancer (CRC). Participants underwent 1.5-T conventional magnetic resonance imaging (MRI) and IVIM-DWI sequence scans with 9 b values (0 to 1,000 s/mm^2) before treatment and at 3 weeks of treatment, and conventional MRI scans were performed at 6 and 12 weeks after the initial treatment. The IVIM-DWI parameters in the tumor target area were extracted using image post-processing software, including perfusion fraction (f), true diffusion coefficient (D), and false diffusion coefficient (D*). The response assessment was based on the Response Evaluation Criteria in Solid Tumors (RECIST) v. 1.1 by measuring the longest tumor diameter on dynamic contrast-enhanced (DCE) T1-weighted images.

Results: According to the RECIST v. 1.1 criteria, the 34 participants were divided into a response group (n=16) and a non-response group (n=18). In the response group, the f value was significantly lowered (P=0.001) and the D value was significantly increased after treatment (P=0.002). In the non-response group, the D value was increased slightly after treatment (P=0.039), and there was no significant difference in the f value and the D* value. In addition, the f value at baseline was significantly greater in the response group than in the non-response group (0.221±0.033 *vs.* 0.175±0.040; P=0.001). The receiver operating characteristic (ROC) curve analysis showed that the percentage change of the f value obtained the largest area under the curve (AUC =0.797), and the AUC obtained by the Fisher's linear discriminant analysis (FLDA) method (Δf & ΔD combination) was 0.819.

Conclusions: The IVIM-DWI parameters (f values and D values) provided effective assessment of the

therapeutic effect of CAPOX combined with bevacizumab in patients with CRLM at an early stage, and the f value of the pre-treatment tumor area was shown to be useful for predicting the treatment response of patients.

Keywords: Colorectal cancer (CRC); liver metastasis; bevacizumab; intravoxel incoherent motion diffusion-weighted imaging (IVIM-DWI); response assessment

Submitted Dec 20, 2021. Accepted for publication Jun 09, 2022.
doi: 10.21037/qims-21-1220
View this article at: https://dx.doi.org/10.21037/qims-21-1220

Introduction

In 2020, there were 19.3 million new cases of cancer and 10 million deaths of cancer patients worldwide, with colorectal cancer (CRC) accounting for 9.8% of the cancers diagnosed and 9.2% of the cancer-related deaths (1). Although the incidence and mortality of CRC in older patients are decreasing, they are increasing in younger adults (2-4). Most patients with CRC are diagnosed at an advanced stage because the majority of clinical symptoms of CRC do not occur until the late stage. About 15–25% of CRC patients have liver metastases (CRLM) at the time of diagnosis, about 50% of patients develop liver metastases throughout the course of the disease (5,6), and the 5-year survival rate of patients with stage IV CRC is only slightly greater than 10% (7). At present, the first-line treatment of advanced CRC is mainly oxaliplatin- or irinotecan-based combination chemotherapy, with epidermal growth factor receptor (EGFR) or vascular endothelial growth factor (VEGF) antagonists added to the first-line treatment if appropriate (8,9). Bevacizumab is a humanized monoclonal antibody against VEGF. It inhibits tumor growth by preventing VEGF from binding to its receptor, resulting in degeneration of the existing tumor vasculature and preventing the development of new blood vessels (10). Currently, the mean overall survival (OS) of metastatic CRC (mCRC) patients is approximately 30 months, twice as high as it was 2 decades ago. Although the improvement in OS may be the result of a combination of multiple factors, the most critical of these has been the introduction of novel biological therapies against epidermal growth factor signaling and angiogenesis, particularly the use of bevacizumab (11). Bevacizumab combined with standard chemotherapy provides treatment benefit to cancer patients regardless of the primary tumor site and rat sarcoma virus (RAS) gene status, especially in RAS wild-type mCRC patients with a right-sided primary tumor (12).

In clinical practice, the response of patients with CRLM after chemotherapy is usually assessed by the Response Evaluation Criteria in Solid Tumors (RECIST) v. 1.1 (13). The RECIST v. 1.1 criteria were developed based on the modification of the World Health Organization (WHO) criteria (14) and are also the most widely used response assessment criteria in clinical practice. However, the limitation of this criterion is the limited sensitivity for assessing the response to treatment according to changes in tumor size, especially when antiangiogenic agents are used in the initial treatment and in the treatment regimen. This is because the mechanism of antiangiogenic agents is to normalize new tumor vessels (10) and thus tumor size may not change in all patients with effective treatment. New evaluation methods have been proposed to better evaluate the response of anti-angiogenic drugs in the treatment of advanced CRC, including computed tomography (CT) morphological criteria (15), the European Organization for Research and Treatment of Cancer (EORTC) criteria (16), and the Positron Emission Tomography (PET) Response Criteria in Solid Tumors (PER-CIST) criteria (17) for PET-CT and dynamic contrast-enhanced (DCE) magnetic resonance imaging (MRI)-based evaluation (18). Although these evaluation methods overcome some of the shortcomings of traditional evaluation methods, their feasibility still needs to be confirmed in well-designed studies with sufficient sample sizes before their wide application in clinical practice.

The current study showed that patients with recurrent, high-grade glioma treated with bevacizumab presented with increased contrast enhancement and dramatically reduced edema without corresponding clinical responses (a phenomenon called “pseudo-response”) (19). With the aim to solve the problem of pseudo response, diffusion-weighted imaging (DWI) is currently proposed to assess tumor response in the presence of antiangiogenic agents

(20-23). The DWI technique can non-invasively detect the diffusion of water molecules and indirectly reflect the microstructural changes of tissues and organs by measuring the apparent diffusion coefficient (ADC) value. The water molecule motion in the tissue, however, is not a simple diffusion, but is limited by the tissue barrier and the incoherent motion produced by blood perfusion, so that the actual measured ADC value is greater than the real diffusion value and fails to accurately reflect water molecule diffusion in the tumor tissue (24). Intravoxel incoherent motion DWI (IVIM-DWI), first proposed by Le Bihan *et al*. in 1986 (25), is an imaging technique that provides quantitative parameters of water molecular motion while reflecting tissue perfusion, so as to more comprehensively analyze tissue diffusion imaging parameters and reveal pathophysiological changes in tumor tissues. Ideally, water molecule motion is a uniform thermal motion, also called Brownian motion, in both velocity and direction. In an organism, due to the constraints of the tissue barrier, the actual motion of water molecules will be limited, that is, diffusion will be restricted (26). DWI is sensitive to the thermally driven random motion of water molecules, and, upon examination, the diffusion of water molecules results in attenuation of the MRI signal (27). Initially, the diffusion effect is described by a monoexponential decay model (28), however, the water molecule motion in the vessel is a pseudo-diffusion process during blood perfusion (29). Blood in the capillary network has incoherent motion at the macroscopic level (25,27,30,31), resulting in a perfusion effect significantly affecting the measurement of the diffusion signal. According to the IVIM theory, diffusion and perfusion are influenced by several tissue properties, including the tissue barrier, volume fraction, velocity of spin diffusion, and the fluid viscosity of the diffusion media (26). The IVIM-DWI parameters reflect the performance of random microscopic motion of water molecules in the intracellular or extracellular in each voxel on MR images, and also present the water molecule motion in hemoperfusion, indicating that IVIM-DWI parameters provide more accurate biological tissue information than DWI. It is assumed that IVIM-DWI criteria perform better than the RECIST v. 1.1 criteria in the early evaluation of the efficacy of antitumor therapy. This prospective study was performed to explore the value of IVIM-DWI in early assessment of the therapeutic effect of chemotherapy combined with anti-angiogenic drugs for CRLM. We present the following article in accordance with the STARD reporting checklist (available at https://qims.amegroups.com/article/view/10.21037/qims-21-1220/rc).

Methods

Participants

The research participants were patients with advanced CRC for whom the primary tumor was located in the right colon regardless of RAS gene status or the left colon with wild-type RAS gene status. Between August 2017 and July 2020, a total of 38 patients were randomly enrolled from Zhongshan Hospital, Xiamen University. All patients had unresectable liver metastases and could tolerate intensive chemotherapy, with an Eastern Cooperative Oncology Group (ECOG) performance status (PS) (32) score of 0–1. All patients were treated with standard chemotherapy plus anti-angiogenic therapy, and the chemotherapy regimen was mainly for the treatment of the primary tumor, with bevacizumab as the anti-tumor/anti-angiogenic drug. Liver metastases with a clear margin and diameter ≥1 cm were included in the study group. Only the largest lesion was selected as target lesion in each patient. The inclusion criteria were as follows: pathologically confirmed adenocarcinoma of the colon or rectum, with unresectable liver metastases and an expected survival time of greater than 3 months; joint confirmation by an imaging doctor with 20 years of experience and an oncologist with 10 years of experience of unresectable liver metastases; no prior treatment (including local or systemic therapy) for liver metastases; presence of at least 1 measurable metastatic lesion (≥1 cm in diameter) in the liver, according to RECIST v. 1.1; an ECOG PS score of 0–1; and, adequate vital organ reserve. The exclusion criteria were as follows: distant metastasis other than in the liver and a previous history of malignant tumors, severe cardiovascular diseases, uncontrolled diabetes, hypertension, bleeding disorders, or unhealed open wounds. The study was conducted in accordance with the Declaration of Helsinki (as revised in 2013). This study was approved by the Ethics Committee of Zhongshan Hospital, Xiamen University (No. 2021-173), and informed consent was provided by all participants.

Treatment regimen

All patients received capecitabine and oxaliplatin (CAPOX) plus bevacizumab (CAPOX + bevacizumab) regimen for chemotherapy. Mode of administration: oxaliplatin was administered at 130 mg/m^2 by continuous intravenous

infusion over 2 h on day 1, followed by intravenous infusion of bevacizumab at a dose of 7.5 mg/kg, with the first infusion time of no less than 90 min and, if well tolerated, the second infusion time was reduced to 60 min. If the patient also tolerated the 60-min infusion, then the duration for all subsequent dosing was reduced to 30 min. Capecitabine was administered at 1,000 mg/m^2 on days 1–14 from the start of chemotherapy, divided into 2 oral doses, with 21 days comprising 1 cycle.

Examination methods

Imaging was performed using a 1.5-T MR Magnetom Symphony Unit (Siemens Healthineers, Erlangen, Germany). Patients fasted for at least 2 h prior to imaging and avoided strenuous exercise until the examination. The imaging was performed in a supine position with the scan covering the entire area of the liver. All patients underwent DWI sequence scans performed with 9 b-values (0, 25, 50, 100, 150, 200, 400, 600, 800, and 1,000 s/mm^2, respectively) before treatment and at 3 weeks after the first treatment; conventional MRI scans were performed before treatment and at 3, 6, and 12 weeks after the first treatment. All examinations were performed within 3 days before the administration of each cycle, and the conventional MRI series included T2-weighted imaging, T1-weighted imaging, and DCE T1-weighted imaging.

Image analysis

The DWI data were processed using the Medical Imaging Interaction Toolkit (MITK; German Cancer Research Center, Heidelberg, Germany; http://www.mitk.org) image post-processing software to obtain the IVIM parameter plot and calculate the IVIM-DWI parameter values corresponding to the tumor area. We selected 1 nodule or mass with maximum diameter >1 cm as the target lesion, and the region of interest (ROI) was selected for the slice with the maximum diameter of the lesion. The ROI delineated on the DWI image was all areas occupied by the tumor lesion. Based on the IVIM concept, the D value, f value, and D* value were calculated according to the following equation by nonlinear biexponential fitting:

$$S_b/S_0 = (1-f)\times\exp(-bD) + f\times\exp(-bD^*) \quad [1]$$

S_0 is the mean signal intensity at time b0, S_b as the signal intensity at time b value greater than 0, the f score is the perfusion fraction, reflecting the proportion of blood perfusion in the diffusion, D is the true diffusion coefficient, reflecting the pure water molecule diffusion, and D* is the false diffusion coefficient, reflecting the water molecule diffusion in blood perfusion.

Response assessment

The longest diameter (LD) of the tumor was measured on axial DCE T1-weighted images, and the tumor reduction rate was calculated according to the maximum tumor diameter among the 3 measurements before and after treatment, according to the formula: tumor reduction rate = (pre-treatment diameter – post-treatment maximum diameter)/pre-treatment diameter × 100%. Responses were categorized according to the RECIST v. 1.1 (13) evaluation criteria: complete response (CR), complete disappearance of the tumor for a period of at least 4 weeks; partial response (PR), ≥30% reduction in the tumor diameter; progressive disease (PD), ≥20% increase in the tumor diameter or occurrence of a new tumor; and stable disease (SD), decrease in the tumor diameter but not meeting the criteria for a PR or increase in the tumor diameter but not meeting the criteria for a PD. According to the RECIST v. 1.1 criteria, patients were divided into the response group (CR + PR) and the non-response group (SD + PD) (33).

Statistical analysis

Statistical analysis was performed using the software SPSS 23.0 (IBM Corp., Armonk, NY, USA) software. Continuous variable data were expressed as mean ± standard deviation. Inter-group comparisons of pre- and post-treatment data were performed using the paired Wilcoxon signed-rank test. Comparisons of data between the response and non-response groups were conducted using the unpaired Mann-Whitney U test. Values of percentage change in the IVIM-DWI parameters (Δf, ΔD, and ΔD*) and the value of percentage change in diameter (ΔLD) observed from baseline to follow-up were also used in the analysis to determine the linear correlations between Δf, ΔD, ΔD*, and ΔLD using Pearson's product-moment correlations. The receiver operating characteristic (ROC) curve analysis was used to evaluate the performance of the values of percentage change in the IVIM parameters before and after treatment to distinguish the responders from the non-responders. The results of combining Δf with ΔD by Fisher's linear discrimination were also used

Table 1 Comparison of tumor size before and after treatment between the response group and the non-response group

Maximum tumor diameter (cm)	Response group (n=16)	Non-response group (n=18)	Total (n=34)
Pre-treatment	5.070±2.418	4.283±3.685	4.939±3.110
Post-treatment	3.243±1.606	4.407±2.572	3.859±2.220
P value	<0.001	0.286	<0.001

The tumor diameter in the table is shown as mean ± standard deviation, and P<0.05 was considered statistically significant (the statistical analysis was performed using the Wilcoxon signed-rank test).

Table 2 Comparison of parameters before and after treatment between the response group and the non-response group

IVIM-DWI parameters	Pre-treatment	Post-treatment	P value
Response group (n=16)			
f	0.221±0.033	0.187±0.030	0.001
D (10^{-3} mm^2/s)	1.246±0.300	1.425±0.280	0.002
D* (10^{-3} mm^2/s)	78.442±19.571	86.716±23.659	0.278
Non-response group (n=18)			
f	0.175±0.040	0.170±0.033	0.248
D (10^{-3} mm^2/s)	1.159±0.189	1.218±0.155	0.039
D* (10^{-3} mm^2/s)	67.903±17.371	78.798±21.018	0.071

Parameters in the table are shown as mean ± standard deviation, and P<0.05 was considered statistically significant (paired data were analyzed using the Wilcoxon signed-rank test). IVIM-DWI, intravoxel incoherent motion diffusion-weighted imaging; f, perfusion fraction; D, true diffusion coefficient; D*, false diffusion coefficient.

for the ROC curve analysis.

Results

Demographics

Between August 2017 and July 2020, a total of 38 patients were randomly enrolled from Zhongshan Hospital, Xiamen University. Excluding 1 patient who withdrew consent and 3 patients who did not complete all scheduled MRI scans, a total of 34 patients (22 males and 12 females, aged 43–80 years, with a mean age of 63 years) were included in the final statistical analyses.

Tumor size

A total of 34 patients with CRLM completed all treatments and examinations and were divided into the response group (n=16; CR =0, PR =16) and the non-response group (n=18; SD =13, PD =5) according to the RECIST v. 1.1 criteria. *Table 1* summarizes the comparison of tumor size before and after treatment between the two groups.

IVIM-DWI parameters

In the response group, the f value was significantly decreased, and the D value was significantly increased (P=0.001 and P=0.002), with the f value decreasing from 0.221±0.033 before treatment to 0.187±0.030 at 3 weeks after the first treatment, and the D value increasing from 1.246±0.300 $\times 10^{-3}$ mm^2/s before treatment to (1.425±0.280) $\times 10^{-3}$ mm^2/s at 3 weeks after the first treatment; however, the difference in the D* value was not statistically significant. The D value also increased slightly after treatment in the non-response group (P=0.039), from (1.159±0.189) $\times 10^{-3}$ mm^2/s before treatment to (1.218±0.155) $\times 10^{-3}$ mm^2/s at 3 weeks after the first treatment, while the difference in the f value and the D* value was not statistically significant. The comparison of the results of each IVIM-WDI parameter before and after treatment between the two groups is summarized in *Table 2*. Box plots of pre- and post-treatment changes in the IVIM-DWI parameters in patients of both groups are shown in *Figure 1*.

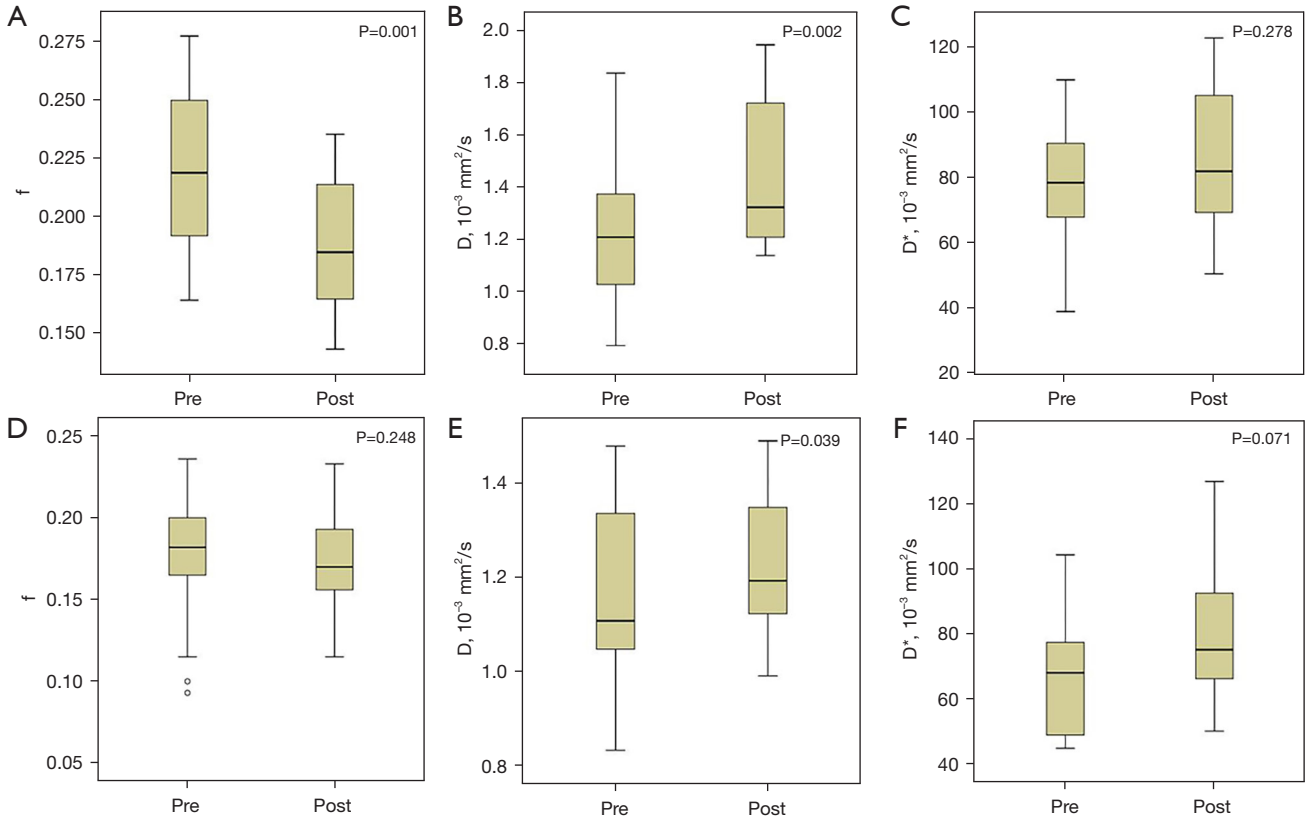

Figure 1 Comparison of IVIM-DWI parameters before and after treatment. (A-C) in the response group. (D-F) in the non-response group. Comparisons between pre- and post-treatment were performed using the Wilcoxon signed-rank test. The middle line corresponds to the median. The lower and upper ends of the box correspond to the first and third quartiles, respectively. The upper and lower edge lines correspond to values within 1.5 times the distance to the quartiles in the box end. Data outside the lower edge line are indicated as "○". Pre, pre-treatment; post, post-treatment; f, perfusion fraction; D, true diffusion coefficient; D*, false diffusion coefficient; IVIM-DWI, intravoxel incoherent motion diffusion-weighted imaging.

Figures 2,3 show the perfusion fraction and true diffusion coefficient of a 61-year-old woman with CRLM, who was classified into the non-response group by RECIST v. 1.1 criteria with no significant change in tumor size before treatment and 21 days after the first treatment. The pre-treatment f value was 0.198, and the post-treatment f value was 0.172; the pre-treatment D value was 1.266×10^{-3} mm^2/s, and the post-treatment D value was 1.333×10^{-3} mm^2/s.

The Mann-Whitney U test revealed that the f value of the response group was significantly greater than that of the non-response group before treatment (0.221±0.033 in the response group *vs.* 0.175±0.040 in the non-response group; P=0.001), indicating a greater possibility of tumor response to anti-angiogenic drugs with richer blood perfusion at baseline. A comparison of the box plots of the pre-treatment IVIM-DWI parameters in the patients of the two groups is shown in *Figure 4*. The results of statistical analysis for each parameter are shown in *Table 3*.

Pearson's product-moment correlation showed a strong correlation between Δf and ΔLD (r=0.714; P<0.001; *Figure 5A*), a moderate correlation between ΔD and ΔLD (r=0.385; P=0.025; *Figure 5B*), and a poor correlation between ΔD* and ΔLD (r=–0.075; P=0.275; *Figure 5C*).

The results of the ROC analysis for the combination of Δf, ΔD, ΔD*, and the Fisher linear discriminant analysis (FLDA) of Δf and ΔD are shown below (*Figure 6*; *Table 4*), and the FLDA had the largest area under the curve (AUC =0.819). Δf had the largest AUC (0.797) when individual parameter was used for analysis. The optimal sensitivity and specificity for each parameter and the corresponding threshold are summarized in *Table 4*.

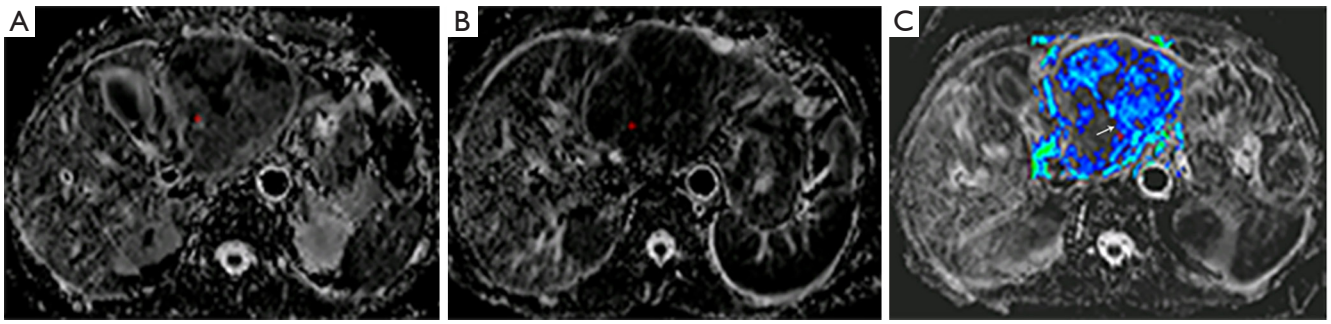

Figure 2 The f maps of a 61-year-old woman with CRLM. (A) The f map of the slice with the maximum diameter of the lesion before treatment. (B) The f map of the slice with the maximum diameter of the lesion after treatment. (C) The subtraction image of the f map. The subtraction image was calculated as the difference of the f maps before and after treatment, and it showed a significant decrease in f values (blue area indicated by the arrow indicates the decrease in f value), suggesting weakened blood perfusion. f, perfusion fraction; CRLM, colorectal cancer liver metastases.

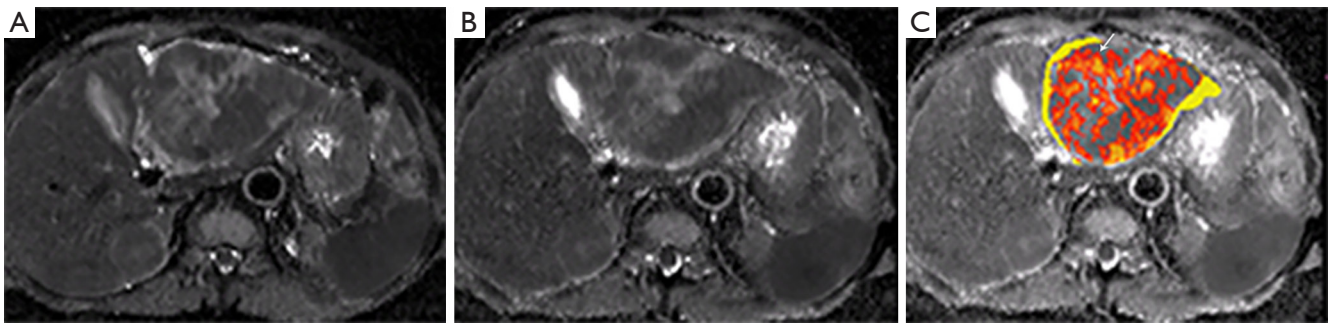

Figure 3 The D maps of a 61-year-old woman with CRLM. (A) The D map of the slice with the maximum diameter of the lesion before treatment. (B) The D map of the slice with the maximum diameter of the lesion after treatment. (C) The subtraction image of the D map. The subtraction image was calculated as the difference of the D maps before and after treatment, and it showed a significant increase in the D values (orange area indicated by the arrow indicates the increase in D values), reflecting increased tumor necrosis. D, true diffusion coefficient; CRLM, colorectal cancer liver metastases.

Discussion

As the most common cancer of the digestive tract, CRC is the second leading cause of cancer death (9.2% of all cancer mortality), and there were an estimated 1.9 million new cases and 910,000 deaths of CRC worldwide in 2020 (34). Although the survival of patients with CRC has greatly improved with advances in treatment, the survival of advanced CRC patients remains unsatisfactory. For these patients, the improvement of systemic chemotherapy regimens and the use of anti-vascular drugs significantly prolong the survival of patients, but the overall response rate needs to be further enhanced. Therefore, the early and accurate assessment of a patient's treatment response is of great significance. The RECIST v. 1.1 (13) standard is still the most important and widely used image-based tumor response evaluation standard for liver tumors all over the world, but it still has obvious limitations. For example, such a standard assumes that all lesions are spherical and their size will uniformly decrease or increase, without considering the existence of necrosis. Targeted therapy and local therapy may lead to the reduction of tumor blood supply and local necrosis. On imaging, the enhancement of the tumor is weakened, yet the size or volume of the tumor does not change significantly, which can lead to misjudgment of tumor treatment efficacy (35). Using IVIM-DWI can not only identify the changes of tumor size but also additional quantitative information about tissue microcirculation perfusion. It can more accurately and truly reflect the pathophysiological changes inside the tumor, thus making

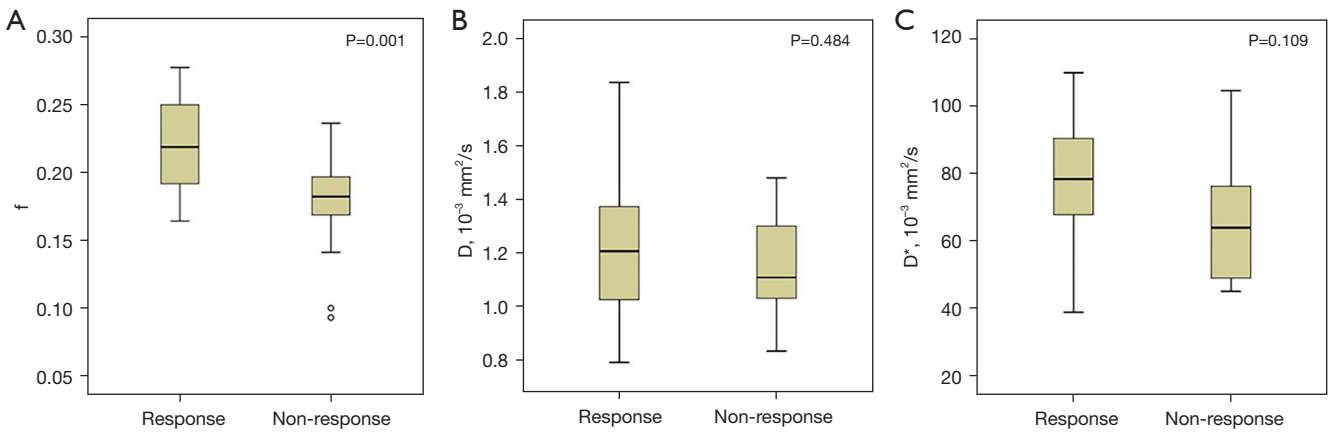

Figure 4 Comparison of IVIM-DWI parameters before treatment between the response group and the non-response group. (A) Comparison of f value. (B) Comparison of D value. (C) Comparison of D* value. The comparison of the IVIM-DWI parameters between the response group and the non-response group was performed using the Mann-Whitney U test. The middle line corresponds to the median. The lower and upper ends of the box correspond to the first and third quartiles, respectively. The upper and lower edge lines correspond to values within 1.5 times the distance to the quartiles in the box end. Data outside the lower edge line are indicated as "○". f, perfusion fraction; D, true diffusion coefficient; D*, false diffusion coefficient; IVIM-DWI, intravoxel incoherent motion diffusion-weighted imaging.

Table 3 Comparison of parameters before treatment between the response group and the non-response group

IVIM-DWI parameters	f	D (10^{-3} mm^2/s)	D* (10^{-3} mm^2/s)
Response group (n=16)	0.221±0.033	1.246±0.300	78.442±19.571
Non-response group (n=18)	0.175±0.040	1.159±0.189	67.903±17.371
P value	0.001	0.484	0.109

All parameters in the table are shown as mean ± standard deviation, and P<0.05 was considered statistically significant (using the Mann-Whitney U test). IVIM-DWI, intravoxel incoherent motion diffusion-weighted Imaging; f, perfusion fraction; D, true diffusion coefficient; D*, false diffusion coefficient.

up for the disadvantages of the RECIST v. 1.1 criteria (36). Our study confirmed the feasibility and superiority of IVIM-DWI as a tumor treatment response evaluation method.

In addition, IVIM-DWI is able to obtain quantitative information about microcirculatory perfusion-related diffusion, which can more accurately and truly reflect the pathophysiological changes inside the tumor, thereby compensating for the disadvantages of traditional DWI. Since the theory was first proposed nearly 30 years ago, research in this field has improved (25). In recent years, a growing number of studies have reported the application of IVIM-DWI to oncology, especially in liver tumors, but the conclusions of studies have been inconsistent, as summarized in a review of the studies in this field (36). Existing evidence shows that tumor tissues have a lower f value and D* value compared with normal liver tissues, while the D value is related to the degree of necrosis of tumor tissues (37,38). The possible reason is that liver tumor tissue has a lower microvessel density (39,40), while malignant tumor vessels are generally immature and structurally incomplete, and slower intraductal blood flow and higher fluid pressure in the lesion result in lower f and D* values than in normal tissue (41-43).

A previous study reported a positive correlation between the percentage of tumor necrosis and the D value, so we have reason to believe that the increase in the D value after treatment reflects an increase in tumor necrosis (38). In our study, the D value was significantly increased in the response group [pre-treatment (1.246±0.300) $\times10^{-3}$ mm^2/s *vs.* post-treatment (1.425±0.280) $\times10^{-3}$ mm^2/s; P=0.002]

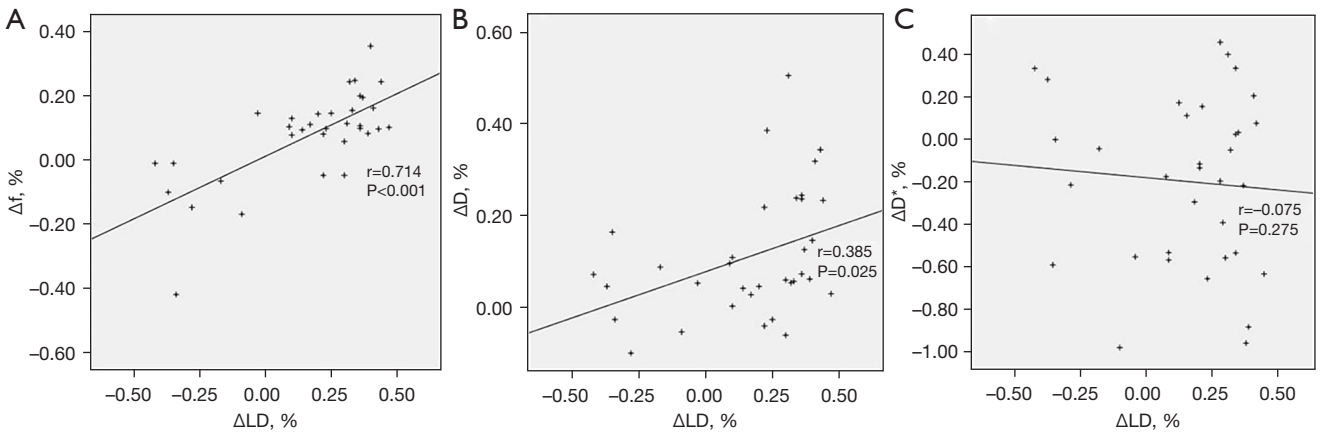

Figure 5 Correlation analysis between percentage change in IVIM-DWI parameters and in the tumor diameter. (A) Correlation analysis between Δf and ΔLD. (B) Correlation analysis between ΔD and ΔLD. (C) Correlation analysis between ΔD* and ΔLD. The correlation analysis of the percentage change in the IVIM-DWI parameters and tumor diameter was performed using the Pearson product moment correlation. Δ, percentage change; f, perfusion fraction; LD, longest diameter; r, Pearson correlation coefficient; D, true diffusion coefficient; D*, false diffusion coefficient; IVIM-DWI, intravoxel incoherent motion diffusion-weighted imaging.

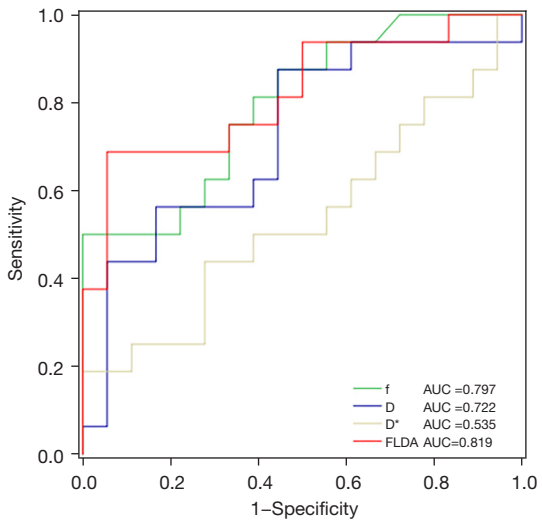

Figure 6 Results of ROC analysis of IVIM-DWI parameters. The green line corresponds to the ROC of the percentage change value of f, the blue line to the ROC of the percentage change value of D, the gray line to the ROC of the percentage change value of D*, the red line to the ROC of FLDA, FLDA = 6.429 × Δf + 2.864 × ΔD − 0.788. f, perfusion fraction; AUC, area under the curve; D, true diffusion coefficient; D*, false diffusion coefficient; FLDA, Fisher linear discriminant analysis; ROC, receiver operating characteristic curve; IVIM-DWI, intravoxel incoherent motion diffusion-weighted imaging.

Table 4 ROC curve analysis using individual parameter percentage change and FLDA

Classifier	AUC	Cut-off value	Sensitivity	Specificity	P value
f	0.797	0.149	0.500	1.000	0.003
D	0.722	0.053	0.875	0.556	0.027
D*	0.535	0.333	0.188	1.000	0.730
FLDA	0.819	0.353	0.688	0.944	0.002

ROC, receiver operating characteristic; FLDA, Fisher's linear discriminant analysis; f, perfusion fraction; D, true diffusion coefficient; D*, false diffusion coefficient; AUC, area under the curve.

and also slightly increased in the non-response group [pre-treatment (1.159±0.189) ×10^{-3} mm^2/s *vs.* post-treatment (1.218±0.155) ×10^{-3} mm^2/s; P=0.039], which indicated that in patients classified as non-response by RECIST v. 1.1 criteria, tumor necrosis was enhanced after treatment. Whether there was a survival benefit in such patients remained unclear, and, unfortunately, we failed to obtain data on patient survival. The results of a study involving the 5-fluorouracil, leucovorin calcium, irinotecan (FOLFIRI) regimen plus bevacizumab in the treatment of CRLM showed a difference, with a significant decrease in the f value but no change in the D value and the D* value at the

end of the first cycle (14 days) of treatment. In addition, it was considered that only the perfusion effect was attenuated and apoptosis had not occurred in such a short time interval, and hence tissue spread was not increased (44). In our study, the f value was significantly lowered at the end of the first cycle (21 days) of treatment (pre-treatment 0.221±0.033 *vs.* post-treatment 0.187±0.033; P=0.001). The D value was also significantly changed, and although we used different treatment regimens (CAPOX + bevacizumab), given that there was no significant difference in efficacy between the 2 treatment regimens in previous studies, it was reasonable to believe that the significant increase in tumor necrosis occurred mainly in the period from 14 days to 21 days after treatment. Additionally, our study also found that before treatment, the f value of patients in the response group was significantly greater than that of those in the non-response group (0.221±0.033 *vs.* 0.175±0.040; P=0.001), which suggested that for CRLM patients treated with chemotherapy combined with bevacizumab, the higher f value before treatment indicated that the blood perfusion of tumor tissue was richer and the possibility of the tumor responding to anti-angiogenic therapy was higher.

Existing studies have shown that the D* value is greatly affected by the signal-to-noise ratio (SNR) and has poor repeatability compared to the good repeatability of the D value and the f value, and the SNR required to achieve good repeatability of D* value is unachievable (45-47). Due to its poor reproducibility, although an increase in the D* value after treatment was observed in both groups of patients in this study, the P value was not statistically significant (P=0.278 in the response group; P=0.071 in the non-response group).

The FLDA is an effective method for distinguishing between 2 types of things by using a linear combination of 2 or more classifiers (48). A study revealed that combining the tumor ADC value with the percentage change in tumor volume using the FLDA method improved the ability to distinguish responders from non-responders after treatment compared with using a single index (49). The decrease in f value and increase in D value observed in our study is due to different mechanisms of drug action, including increased necrosis caused by chemotherapeutic drugs and decreased blood perfusion caused by anti-vascular drugs. Hence, the use of a single parameter to discriminate the therapeutic response of patients may underestimate the effect of the drug, and the use of the FLDA method in combination with the percentage changes in f and D values for therapeutic response discrimination improves the discriminant power.

Although IVIM-DWI shows great potential as an efficacy evaluation tool, the optimal examination time remains unclear. In animal experiments, after the use of vascular disrupting agents, a decrease in the f value and the D* value was observed as early as 4 h after administration, while the D value increased after 24 h (50). Another animal experiment with sorafenib for hepatocellular carcinoma indicated that in the experimental group, an increase in the D value was observed 7 days after treatment and continued to increase thereafter, and the f value decreased 7 days after treatment but increased again at 14 days after treatment and was significantly higher than the baseline value at 21 days after treatment (51). In CRLM patients treated with FOLFIRI plus bevacizumab, a significant decrease in the f value was observed 14 days after the first treatment, but there was no significant change in the D value (44). These findings are different from the results of another study based on combination chemotherapy in patients with CRLM, in which the f value was significantly decreased after the first cycle (14 days) of chemotherapy, while the D value was significantly increased (33). Although the results of various studies have lacked consistency, the discrepancies may be attributed to differences in the examination time point, treatment regimens, and disease types included in each study design, and most of the studies have been based on studies with small sample sizes. The results of this study showed that the f value was significantly reduced and the D value was significantly increased at 3 weeks after treatment, indicating that it is feasible to evaluate the treatment response by IVIM at 3 weeks after the first treatment.

In our study, the ROI selection covered the entire tumor area and did not deliberately avoid blood vessels with necrotic areas. Firstly, in some tumor lesions, it is very difficult to avoid both blood vessels and necrotic areas and to select ROIs with the same sized area on images at different stages, especially when the tumor size and shape change. Secondly, it is difficult to select only some areas as ROIs to reflect the overall real treatment response of tumors. From previous studies, we know that the f value is related to microvessel density, and the D value is related to tumor necrosis. It is unknown whether this relationship prevails under the deliberate avoidance of examining blood vessels and necrotic areas.

There were some limitations to this study. Firstly, for the liver, IVIM modeling of the perfusion component is constrained by the diffusion component, and a reduced D measure leads to artificially higher f and D* values. The influencing factors include age, hepatic steatosis, and

hepatic fibrosis, and this problem is not easily solvable by a better fitting approach, by high signal-to-noise images, or by an extensive array of b-value images. Further research to better separate the diffusion component and the perfusion component should be pursued. Another possible approach would be that, if the reference values of the IVIM diffusion and perfusion components are already known with standardized data acquisition, then we may be able to understand how these constraints can be computationally compensated for by each target tissue (52-56). Secondly, we must evaluate the treatment response of patients using the RECIST v. 1.1 criteria. We already know that RECIST v. 1.1 may not accurately identify some patients who respond to treatment, especially when combined with anti-vascular drugs, but we have no better way to finally confirm whether these patients really benefit from treatment. Pathological analysis may be a good choice, but unfortunately in patients with advanced cancer, we failed to obtain tumor samples due to the interests of the patients. Another good option is through survival data; however, obtaining complete survival data is equally difficult. Furthermore, we only performed IVIM-DWI at 21 days before and after treatment and did not obtain parameter data at other time points, especially at earlier time points. Although our findings suggest the feasibility of performing IVIM-DWI at 21 days, whether this is the optimal time point still needs further investigation. Finally, consistent with other studies on IVIM-DWI, our study had a small sample size and did not include patients treated with chemotherapy alone. Future studies should expand the sample size and include patients treated with chemotherapy alone and without anti-vascular drugs to confirm that the above findings are more broadly applicable in the clinical setting.

Conclusions

The f and D of IVIM-DWI parameters provide opportunity for the early assessment of the therapeutic response to chemotherapy combined with bevacizumab in patients with CRLM. The f at baseline is beneficial for predicting the treatment response of CRLM patients.

Acknowledgments

Funding: This work was supported by the Key Projects of Natural Science Foundation of Fujian Province (No. 2014D022); the Young and Middle-Aged Backbone Talents Training Program of Fujian Provincial Health Commission (No. 2019-ZQNB-29); Medical and Health Science and Technology Plan Project of Xiamen, China (No. 3502Z20194018); Youth Innovation Projects of Natural Science Foundation of Fujian Province (No. 2020J05287).

Footnote

Reporting Checklist: The authors have completed the STARD reporting checklist. Available at https://qims.amegroups.com/article/view/10.21037/qims-21-1220/rc

Conflicts of Interest: All authors have completed the ICMJE uniform disclosure form (available at https://qims.amegroups.com/article/view/10.21037/qims-21-1220/coif). The authors have no conflicts of interest to declare.

Ethical Statement: The authors are accountable for all aspects of the work in ensuring that questions related to the accuracy or integrity of any part of the work are appropriately investigated and resolved. The study was conducted in accordance with the Declaration of Helsinki (as revised in 2013). This study was approved by the Ethics Committee of Zhongshan Hospital, Xiamen University (No. 2021-173) and informed consent was provided by all participants.

References

1. Sung H, Ferlay J, Siegel RL, Laversanne M, Soerjomataram I, Jemal A, Bray F. Global Cancer Statistics 2020: GLOBOCAN Estimates of Incidence and Mortality Worldwide for 36 Cancers in 185 Countries. CA Cancer J Clin 2021;71:209-49.
2. Lucente P, Polansky M. Colorectal cancer rates are rising in younger adults. JAAPA 2018;31:10-1.
3. Chittleborough TJ, Gutlic I, Pearson JF, Watson A, Bhatti LA, Buchwald P, Potter JD, Wakeman C, Eglinton T, Frizelle F. Increasing Incidence of Young-Onset Colorectal

Carcinoma A 3-Country Population Analysis. Dis Colon Rectum 2020;63:903-10.
4. Dekker E, Tanis PJ, Vleugels JLA, Kasi PM, Wallace MB. Colorectal cancer. Lancet 2019;394:1467-80.
5. Constantinidou A, Cunningham D, Shurmahi F, Asghar U, Barbachano Y, Khan A, Mudan S, Rao S, Chau I. Perioperative chemotherapy with or without bevacizumab in patients with metastatic colorectal cancer undergoing liver resection. Clin Colorectal Cancer 2013;12:15-22.
6. van der Geest LG, Lam-Boer J, Koopman M, Verhoef C, Elferink MA, de Wilt JH. Nationwide trends in incidence, treatment and survival of colorectal cancer patients with synchronous metastases. Clin Exp Metastasis 2015;32:457-65.
7. Brenner H, Kloor M, Pox CP. Colorectal cancer. Lancet 2014;383:1490-502.
8. Hurwitz H, Fehrenbacher L, Novotny W, Cartwright T, Hainsworth J, Heim W, Berlin J, Baron A, Griffing S, Holmgren E, Ferrara N, Fyfe G, Rogers B, Ross R, Kabbinavar F. Bevacizumab plus irinotecan, fluorouracil, and leucovorin for metastatic colorectal cancer. N Engl J Med 2004;350:2335-42.
9. Kabbinavar FF, Schulz J, McCleod M, Patel T, Hamm JT, Hecht JR, Mass R, Perrou B, Nelson B, Novotny WF. Addition of bevacizumab to bolus fluorouracil and leucovorin in first-line metastatic colorectal cancer: results of a randomized phase II trial. J Clin Oncol 2005;23:3697-705.
10. Jain RK. Normalization of tumor vasculature: an emerging concept in antiangiogenic therapy. Science 2005;307:58-62.
11. Kopetz S, Chang GJ, Overman MJ, Eng C, Sargent DJ, Larson DW, Grothey A, Vauthey JN, Nagorney DM, McWilliams RR. Improved survival in metastatic colorectal cancer is associated with adoption of hepatic resection and improved chemotherapy. J Clin Oncol 2009;27:3677-83.
12. You XH, Jiang YH, Fang Z, Sun F, Li Y, Wang W, Xia ZJ, Wang XZ, Ying HQ. Chemotherapy plus bevacizumab as an optimal first-line therapeutic treatment for patients with right-sided metastatic colon cancer: a meta-analysis of first-line clinical trials. ESMO Open 2020;4:e000605.
13. Eisenhauer EA, Therasse P, Bogaerts J, Schwartz LH, Sargent D, Ford R, Dancey J, Arbuck S, Gwyther S, Mooney M, Rubinstein L, Shankar L, Dodd L, Kaplan R, Lacombe D, Verweij J. New response evaluation criteria in solid tumours: revised RECIST guideline (version 1.1). Eur J Cancer 2009;45:228-47.
14. World Health Organization. WHO handbook for reporting results of cancer treatment. Geneva: World Health Organization, 1979.
15. Chun YS, Vauthey JN, Boonsirikamchai P, Maru DM, Kopetz S, Palavecino M, Curley SA, Abdalla EK, Kaur H, Charnsangavej C, Loyer EM. Association of computed tomography morphologic criteria with pathologic response and survival in patients treated with bevacizumab for colorectal liver metastases. JAMA 2009;302:2338-44.
16. Young H, Baum R, Cremerius U, Herholz K, Hoekstra O, Lammertsma AA, Pruim J, Price P. Measurement of clinical and subclinical tumour response using [18F]-fluorodeoxyglucose and positron emission tomography: review and 1999 EORTC recommendations. European Organization for Research and Treatment of Cancer (EORTC) PET Study Group. Eur J Cancer 1999;35:1773-82.
17. Wahl RL, Jacene H, Kasamon Y, Lodge MA. From RECIST to PERCIST: Evolving Considerations for PET response criteria in solid tumors. J Nucl Med 2009;50 Suppl 1:122S-50S.
18. De Bruyne S, Van Damme N, Smeets P, Ferdinande L, Ceelen W, Mertens J, Van de Wiele C, Troisi R, Libbrecht L, Laurent S, Geboes K, Peeters M. Value of DCE-MRI and FDG-PET/CT in the prediction of response to preoperative chemotherapy with bevacizumab for colorectal liver metastases. Br J Cancer 2012;106:1926-33.
19. Sorensen AG, Batchelor TT, Wen PY, Zhang WT, Jain RK. Response criteria for glioma. Nat Clin Pract Oncol 2008;5:634-44.
20. Chenevert TL, Stegman LD, Taylor JM, Robertson PL, Greenberg HS, Rehemtulla A, Ross BD. Diffusion magnetic resonance imaging: an early surrogate marker of therapeutic efficacy in brain tumors. J Natl Cancer Inst 2000;92:2029-36.
21. Gerstner ER, Frosch MP, Batchelor TT. Diffusion magnetic resonance imaging detects pathologically confirmed, nonenhancing tumor progression in a patient with recurrent glioblastoma receiving bevacizumab. J Clin Oncol 2010;28:e91-3.
22. Pope WB, Kim HJ, Huo J, Alger J, Brown MS, Gjertson D, Sai V, Young JR, Tekchandani L, Cloughesy T, Mischel PS, Lai A, Nghiemphu P, Rahmanuddin S, Goldin J. Recurrent glioblastoma multiforme: ADC histogram analysis predicts response to bevacizumab treatment. Radiology 2009;252:182-9.
23. Jain R, Scarpace LM, Ellika S, Torcuator R, Schultz LR, Hearshen D, Mikkelsen T. Imaging response criteria for recurrent gliomas treated with bevacizumab: role of

diffusion weighted imaging as an imaging biomarker. J Neurooncol 2010;96:423-31.
24. Dia AA, Hori M, Onishi H, Sakane M, Ota T, Tsuboyama T, Tatsumi M, Okuaki T, Tomiyama N. Application of non-Gaussian water diffusional kurtosis imaging in the assessment of uterine tumors: A preliminary study. PLoS One 2017;12:e0188434.
25. Le Bihan D, Breton E, Lallemand D, Grenier P, Cabanis E, Laval-Jeantet M. MR imaging of intravoxel incoherent motions: application to diffusion and perfusion in neurologic disorders. Radiology 1986;161:401-7.
26. Le Bihan D, Johansen-Berg H. Diffusion MRI at 25: exploring brain tissue structure and function. Neuroimage 2012;61:324-41.
27. Le Bihan D, Breton E, Lallemand D, Aubin ML, Vignaud J, Laval-Jeantet M. Separation of diffusion and perfusion in intravoxel incoherent motion MR imaging. Radiology 1988;168:497-505.
28. Koh DM, Collins DJ. Diffusion-weighted MRI in the body: applications and challenges in oncology. AJR Am J Roentgenol 2007;188:1622-35.
29. Le Bihan D. What can we see with IVIM MRI? Neuroimage 2019;187:56-67.
30. Le Bihan D, Turner R. The capillary network: a link between IVIM and classical perfusion. Magn Reson Med 1992;27:171-8.
31. Le Bihan D, Turner R, Moonen CT, Pekar J. Imaging of diffusion and microcirculation with gradient sensitization: design, strategy, and significance. J Magn Reson Imaging 1991;1:7-28.
32. Oken MM, Creech RH, Tormey DC, Horton J, Davis TE, McFadden ET, Carbone PP. Toxicity and response criteria of the Eastern Cooperative Oncology Group. Am J Clin Oncol 1982;5:649-55.
33. Kim JH, Joo I, Kim TY, Han SW, Kim YJ, Lee JM, Han JK. Diffusion-Related MRI Parameters for Assessing Early Treatment Response of Liver Metastases to Cytotoxic Therapy in Colorectal Cancer. AJR Am J Roentgenol 2016;207:W26-32.
34. Siegel RL, Miller KD, Goding Sauer A, Fedewa SA, Butterly LF, Anderson JC, Cercek A, Smith RA, Jemal A. Colorectal cancer statistics, 2020. CA Cancer J Clin 2020;70:145-64.
35. Forner A, Ayuso C, Varela M, Rimola J, Hessheimer AJ, de Lope CR, Reig M, Bianchi L, Llovet JM, Bruix J. Evaluation of tumor response after locoregional therapies in hepatocellular carcinoma: are response evaluation criteria in solid tumors reliable? Cancer 2009;115:616-23.
36. Tao YY, Zhou Y, Wang R, Gong XQ, Zheng J, Yang C, Yang L, Zhang XM. Progress of intravoxel incoherent motion diffusion-weighted imaging in liver diseases. World J Clin Cases 2020;8:3164-76.
37. Vandecaveye V, Michielsen K, De Keyzer F, Laleman W, Komuta M, Op de beeck K, Roskams T, Nevens F, Verslype C, Maleux G. Chemoembolization for hepatocellular carcinoma: 1-month response determined with apparent diffusion coefficient is an independent predictor of outcome. Radiology 2014;270:747-57.
38. Chiaradia M, Baranes L, Van Nhieu JT, Vignaud A, Laurent A, Decaens T, Charles-Nelson A, Brugières P, Katsahian S, Djabbari M, Deux JF, Sobhani I, Karoui M, Rahmouni A, Luciani A. Intravoxel incoherent motion (IVIM) MR imaging of colorectal liver metastases: are we only looking at tumor necrosis? J Magn Reson Imaging 2014;39:317-25.
39. Lee HJ, Rha SY, Chung YE, Shim HS, Kim YJ, Hur J, Hong YJ, Choi BW. Tumor perfusion-related parameter of diffusion-weighted magnetic resonance imaging: correlation with histological microvessel density. Magn Reson Med 2014;71:1554-8.
40. Iima M, Reynaud O, Tsurugizawa T, Ciobanu L, Li JR, Geffroy F, Djemai B, Umehana M, Le Bihan D. Characterization of glioma microcirculation and tissue features using intravoxel incoherent motion magnetic resonance imaging in a rat brain model. Invest Radiol 2014;49:485-90.
41. Bäuerle T, Seyler L, Münter M, Jensen A, Brand K, Fritzsche KH, Kopp-Schneider A, Schüssler M, Schlemmer HP, Stieltjes B, Ganten M. Diffusion-weighted imaging in rectal carcinoma patients without and after chemoradiotherapy: a comparative study with histology. Eur J Radiol 2013;82:444-52.
42. Kim S, Decarlo L, Cho GY, Jensen JH, Sodickson DK, Moy L, Formenti S, Schneider RJ, Goldberg JD, Sigmund EE. Interstitial fluid pressure correlates with intravoxel incoherent motion imaging metrics in a mouse mammary carcinoma model. NMR Biomed 2012;25:787-94.
43. Gade TP, Buchanan IM, Motley MW, Mazaheri Y, Spees WM, Koutcher JA. Imaging intratumoral convection: pressure-dependent enhancement in chemotherapeutic delivery to solid tumors. Clin Cancer Res 2009;15:247-55.
44. Granata V, Fusco R, Catalano O, Filice S, Amato DM, Nasti G, Avallone A, Izzo F, Petrillo A. Early Assessment of Colorectal Cancer Patients with Liver Metastases Treated with Antiangiogenic Drugs: The Role of Intravoxel Incoherent Motion in Diffusion-Weighted

Imaging. PLoS One 2015;10:e0142876.
45. Li YT, Cercueil JP, Yuan J, Chen W, Loffroy R, Wáng YX. Liver intravoxel incoherent motion (IVIM) magnetic resonance imaging: a comprehensive review of published data on normal values and applications for fibrosis and tumor evaluation. Quant Imaging Med Surg 2017;7:59-78.
46. Andreou A, Koh DM, Collins DJ, Blackledge M, Wallace T, Leach MO, Orton MR. Measurement reproducibility of perfusion fraction and pseudodiffusion coefficient derived by intravoxel incoherent motion diffusion-weighted MR imaging in normal liver and metastases. Eur Radiol 2013;23:428-34.
47. Kakite S, Dyvorne H, Besa C, Cooper N, Facciuto M, Donnerhack C, Taouli B. Hepatocellular carcinoma: short-term reproducibility of apparent diffusion coefficient and intravoxel incoherent motion parameters at 3.0T. J Magn Reson Imaging 2015;41:149-56.
48. Fisher RA. The use of multiple measurements in taxonomic problems. Annals of Eugenics 1936;7:179-88.
49. Schneider MJ, Cyran CC, Nikolaou K, Hirner H, Reiser MF, Dietrich O. Monitoring early response to anti-angiogenic therapy: diffusion-weighted magnetic resonance imaging and volume measurements in colon carcinoma xenografts. PLoS One 2014;9:e106970.
50. Joo I, Lee JM, Han JK, Choi BI. Intravoxel incoherent motion diffusion-weighted MR imaging for monitoring the therapeutic efficacy of the vascular disrupting agent CKD-516 in rabbit VX2 liver tumors. Radiology 2014;272:417-26.
51. Yang SH, Lin J, Lu F, Han ZH, Fu CX, Lv P, Liu H, Gao DM. Evaluation of antiangiogenic and antiproliferative effects of sorafenib by sequential histology and intravoxel incoherent motion diffusion-weighted imaging in an orthotopic hepatocellular carcinoma xenograft model. J Magn Reson Imaging 2017;45:270-80.
52. Huang H, Zheng CJ, Wang LF, Che-Nordin N, Wáng YXJ. Age and gender dependence of liver diffusion parameters and the possibility that intravoxel incoherent motion modeling of the perfusion component is constrained by the diffusion component. NMR Biomed 2021;34:e4449.
53. Wáng YXJ. Observed paradoxical perfusion fraction elevation in steatotic liver: An example of intravoxel incoherent motion modeling of the perfusion component constrained by the diffusion component. NMR Biomed 2021;34:e4488.
54. Wáng YXJ. Mutual constraining of slow component and fast component measures: some observations in liver IVIM imaging. Quant Imaging Med Surg 2021;11:2879-87.
55. Wáng YXJ. A reduction of perfusion can lead to an artificial elevation of slow diffusion measure: examples in acute brain ischemia MRI intravoxel incoherent motion studies. Ann Transl Med 2021;9:895.
56. Xiao BH, Huang H, Wang LF, Qiu SW, Guo SW, Wáng YXJ. Diffusion MRI Derived per Area Vessel Density as a Surrogate Biomarker for Detecting Viral Hepatitis B-Induced Liver Fibrosis: A Proof-of-Concept Study. SLAS Technol 2020;25:474-83.

Cite this article as: Wu H, Li B, Yang Z, Ji H, Guo Y, Lin J, Wang X. Intravoxel incoherent motion diffusion-weighted imaging for early assessment of combined anti-angiogenic/chemotherapy for colorectal cancer liver metastases. Quant Imaging Med Surg 2022;12(9):4587-4600. doi: 10.21037/qims-21-1220

